International Journal of Current Engineering and Technology
E-ISSN 2277 – 4106, P-ISSN 2347 – 5161

Available at http://inpressco.com/category/ijcet

Research Article

Modeling & Simulation of Three Phase Grid Connected Solar PV System

Pradeep Rai* and Roshan Nayak

Electrical Engineering Department, SHUATS, Allahabad, India

Received 04 April 2018, Accepted 05 June 2018, Available online 09 June 2018, **Vol.8, No.3 (May/June 2018)**

Abstract

This paper proposes a nonlinear control methodology for three phase grid connected of PV generator. It consists of a PV arrays; a voltage source inverter, a grid filter and an electric grid. The controller objectives are threefold: i) ensuring the Maximum power point tracking (MPPT) in the side of PV panels, ii) guaranteeing a power factor unit in the side of the grid, iii) ensuring the global asymptotic stability of the closed loop system. Based on the nonlinear model of the whole system, the controller is carried out using a Lyapunov approach. It is formally shown, using a theoretical stability analysis and simulation results that the proposed controller meets all the objectives.

Keywords: *Solar PV System, DC link, Three Phase Inverter &converter*

1. Introduction

With rising concerns about global warming and more since the last spike in oil prices that will cease to increase, renewable energy, long considered a useful adjunct course. Today, oil and gas are still relatively cheap. With the scarcity of raw materials, the price of fossil fuels will continue to rise. At the same time that renewable energy price should decrease mainly due to technological advances and production in larger series. This is why the PV system has a great bright future in the forthcoming years. The PV grid connected systems have become one of the most important applications of solar energy (Chiang, 1998; Doncker, 2007; Enslin, 1991). Different control strategy for three phase grid connected of PV modules has been largely dealt with in the specialist literature in the last few years (Anthony Purcell, 2001; Cristian Lascu, 2000) Nevertheless, good integration of medium or large PV system in the grid may therefore require additional functionality from the inverter, such as control of reactive power. Moreover, the increase in the average size of a PV system may lead to new strategies such as eliminating the DC-DC converter which is usually placed between the PV generator and inverter, and moving the MPPT to the inverter, which leads to increased simplicity, overall efficiency and a cost reduction. These two features are present in the three phase inverter that is presented here, with the addition of a P&O MPPT algorithm. The present paper is then focusing on the problem of controlling three phase grid-connected PV power generation systems. The control objectives are threefold: (i) global asymptotic stability of the whole closed-loop control system; (ii) achievement of the MPPT for the PV array; and (iii) ensuring a grid connection with unity Power Factor (PF). These objectives should be achieved in spite the climatic variables (temperature and radiation) changes. To this end, a nonlinear controller is developed using Lyapunov design technique. A theoretical analysis is developed to show that the controller actually meets its objectives a fact that is confirmed by simulation. The paper is organized as follows: the three phase grid connected PV system is described and modeled in Section II. Section III is devoted to controller design and analysis. The controller tracking performances are illustrated by numerical simulation in Section IV.

2. System Description and Modelling

A. System description

The main circuit of three-phase grid-connected photovoltaic system is shown in Fig.1. It consists of a PV arrays; a DC link capacitor *C*; a three phase inverter (including six power semiconductors) that is based upon to ensure a DC-AC power conversion and unity power factor; a inductor filter *L* with its ESR resistance *r,* and an electric grid. The control inputs of the system are a PWM signals *ua*, *ub* and *uc* taking values in the set {0,1}. The grid voltages *ega*, *egb* and *egc* constitute a three phase balanced system.

*Corresponding author's ORCID ID: 0000-0001-9309-4525
DOI: https://doi.org/10.14741/ijcet/v.8.3.22

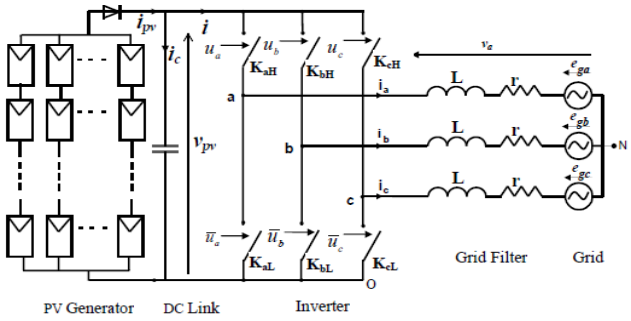

Fig.1: Three phase grid connected PV system

B. PV array model

An equivalent circuit for a PV cell is shown in Fig. 2. Its current characteristic can be found in many places (Ding, 2010; Doncker, 2007) and presents the following expression

$$I = I_{ph} - I_{sat}\left[\exp\left(\frac{q(V+IR_s)}{AkT}\right)-1\right]-\frac{V+IR_s}{R_p} \quad (1)$$

Where,

$$\begin{cases} I_{sat} = I_{satr}\left[\frac{T}{T_r}\right]^3 \exp\left[\frac{qE_{G0}}{Ak}\left(\frac{1}{T_r}-\frac{1}{T}\right)\right] \\ I_{ph} = \left[I_{phr} + K_I(T-298)\right]\lambda \end{cases} \quad (2)$$

The meaning and typical values of the parameters given by (1) and (2) can be found in many places (Boldue, 1993; Bragard, 2010; Ertl, H. J, 2002), A is diode ideal factor, k is Boltzmann constant k = 1.38×10^{-23} J / K , T is temperature on absolute scale in K, q is electron charge q = 1.6 $\times10^{-19}C$ and λ is the radiation in kW/m^2, I_{phr} is the short-circuit current at 298 K and 1 kW/m^2, KI = 0.0017 A/K is the current temperature coefficient at I_{phr}, $EG0$ is the band gap for silicon, Tr = 301.18K is reference temperature, I_{satr} is cell saturation current at Tr. PV array consists of Ns cells in series formed the panel and of Np panels in parallel according to the rated power required. The output voltage and current can be given by the following equations:

$$v_{pv} = N_s(V_d - R_s I) \quad (3)$$

$$i_{pv} = N_p I \quad (4)$$

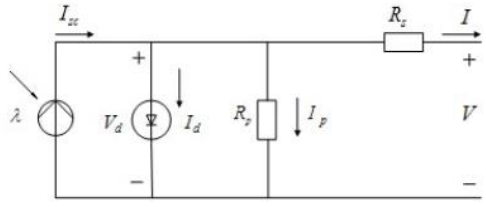

Fig.2 The equivalent circuit for a PV cell

The photovoltaic generator considered in this paper consists of several NU-183E1 modules. The corresponding electrical characteristics of PV modules are shown in Table I. The associated power-voltage (P-V) characteristics under changing climatic conditions (temperature and radiation) are shown in Figs. 3 and 4. This highlights the Maximum Power Point (MPP) M1 to M5, whose coordinates are given in Table III. The data in Table I to Table III will be used for simulation.

Table II shows the main characteristics of the PV array, designed using Sharp NU-183E1 modules connected in a proper series-parallel, making up a peak installed power of 71.75 kW. As there is no DC-DC converter between the PV generator and the inverter, the PV array configuration should be chosen such that the output voltage of the photovoltaic generator is adapted to the requirements of the inverter.

In this case a 380V grid has been chosen, so the inverter would need at least 570V DC bus in order to be able to operate correctly. The minimum number of modules connected in series should be determined by the value of the minimum DC bus voltage and the worst case climatic conditions. The PV array was found to require 28 series connected modules per string.

Table 1: Electrical Specifications For The Solar Module NU-183E1

Parameter	Symbol	Value
Maximum Power	P_m	**183 W**
Shortcircuit current	I_{scr}	**8.48 A**
Opencircuit voltage	V_{OC}	**31.1 V**
Maximum power voltage	V_m	**29.9 V**
Maximum power current	I_m	**7.66 A**
Number of parallel modules	N_p	**1**
Number of series modules	N_s	**48**

Table 2: PV Array Specifications Using Sharpnu-183E1

Parameter	Symbol	Value
Total peak power	P_m	**71.75 kW**
Number of series strings	N_S	**28**
Number of parallel	N_P	**14**
Number of PV panels	N	**432**
Voltage in maximum power	V_m	**664**
Current peak	I_m	**108 A**

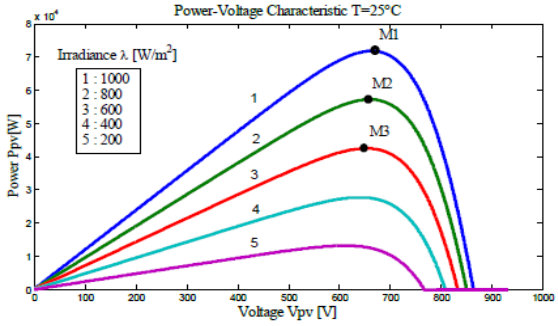

Fig.3: (P-V) characteristics of The PV Generator (NP=14 And NS=28) with constant temperature and varying radiation

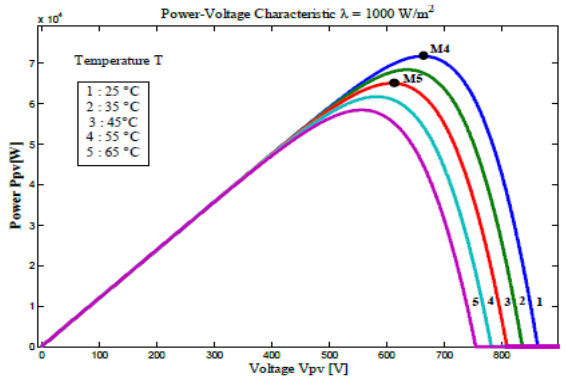

Fig.4: (P-V) characteristics of The PV Generator (*NP*=14 And *NS*=28) with constant radiation and varying temperature

Table 3: Maximum Power Points (MPP) In Fig.3 And Fig.4

MPP	Vm [V]	Pm [KW]
M1	664.21	71.77
M2	661.04	57.21
M3	654.34	42.50
M4	664.21	71.77
M5	610.63	65.08

C. Modelling of three-phase Grid-Connected PV System

The state-space model of a three-phase grid-connected photovoltaic system shown in Fig. 1 can be obtained by the dynamic equations described as follows:

$$\frac{d}{dt}\begin{bmatrix} i_a \\ i_b \\ i_c \end{bmatrix} = -\frac{r}{L}\begin{bmatrix} i_a \\ i_b \\ i_c \end{bmatrix} + \frac{v_{pv}}{3L}\begin{bmatrix} 2 & -1 & -1 \\ -1 & 2 & -1 \\ -1 & -1 & 2 \end{bmatrix}\begin{bmatrix} u_a \\ u_b \\ u_c \end{bmatrix} - \frac{1}{L}\begin{bmatrix} e_{ga} \\ e_{gb} \\ e_{gc} \end{bmatrix} \quad (5a)$$

$$\frac{d}{dt}v_{pv} = \frac{1}{C}i_{pv} - \frac{1}{C}\left(u_a i_a + u_b i_b + u_c i_c\right) \quad (5b)$$

Applying the d-q transformation to (5a-b), one obtains the following instantaneous model in d-q frame

Where,

$$u_i = \begin{cases} 1 \rightarrow K_{iH} : on;\ K_{iL} : off \\ 0 \rightarrow K_{iH} : off;\ K_{iL} : on \end{cases}$$

Applying the d-q transformation to (5a-b), one obtains the following instantaneous model in d-q frame

$$\frac{d}{dt}i_d = -\frac{r}{L}i_d + \omega\, i_q + \frac{v_{pv}}{L}u_d - \frac{1}{L}e_{gd} \quad (6a)$$

$$\frac{d}{dt}i_q = -\frac{r}{L}i_q - \omega\, i_d + \frac{v_{pv}}{L}u_q - \frac{1}{L}e_{gq} \quad (6b)$$

$$\frac{d}{dt}v_{pv} = -\frac{3}{2C}\left(u_d i_d + u_q i_q\right) + \frac{1}{C}i_{pv} \quad (6c)$$

Where,

$$\left[i_{dqo}\right] = \left[T_{abc}^{dqo}\right]\left[i_{abc}\right] : \left[e_{gdqo}\right] = \left[T_{abc}^{dqo}\right]\left[e_{gabc}\right]$$

$$\left[u_{dqo}\right] = \left[T_{abc}^{dqo}\right]\left[u_{abc}\right]$$

The transformation matrix T_{abc}^{dqo} is given by

$$T_{abc}^{dqo} = \frac{2}{3}\begin{bmatrix} \sin(\omega t) & \sin(\omega t - \frac{2\pi}{3}) & \sin(\omega t - \frac{4\pi}{3}) \\ \cos(\omega t) & \cos(\omega t - \frac{2\pi}{3}) & \cos(\omega t - \frac{4\pi}{3}) \\ \frac{1}{2} & \frac{1}{2} & \frac{1}{2} \end{bmatrix} \quad (7)$$

$$P = \frac{3}{2}\left(e_{gd} i_d + e_{gq} i_q\right) \quad (8a)$$

$$Q = \frac{3}{2}\left(e_{gq} i_d - e_{gd} i_q\right) \quad (8b)$$

Where P is active power and Q is reactive power. In synchronous d-q rotating, *eq=0*, therefore

$$P = \frac{3}{2}e_{gd} i_d \quad (9a)$$

$$Q = -\frac{3}{2}e_{gd} i_q \quad (9b)$$

The active power P can be controlled by the current *id* and the reactive power Q can be controlled by the current *iq*.

3. Controller Design and Analysis

With the aim of design an appropriate control for the model (6) described in previous section, the control objectives, the control design and stability analysis will be investigated in this Section, taking into account the nonlinear feature and the multi-input multi-output (MIMO) aspect of the system

A. Control objectives

In order to define the control strategy, first one has to establish the control objectives, which can be formulated as follows:

i) Maximum power point tracking (MPPT) of PV arrays,
ii) Unity power factor (PF) in the grid,
iii) Asymptotic stability of the whole system.

B. Nonlinear control design

Once the control objectives are defined, as the MIMO system is highly nonlinear, a Lyapunov based nonlinear control is proposed. The first control objective is to enforce the real power *P* to track the maximum power point *PM*. It's already point out, that this power can be controlled by the d-axis current *id*. In this paper the MPPT algorithm based on the Perturb and Observe (P&O) technique (11] is resorted to generate the reference signal *idref* of the current *id* so that if *id* = *idref* the active power *P* tracks its maximum value i.e. *P* = *PM*.

Lets us first introduce the following error

$$e_1 = i_d - i_{dref} \tag{10}$$

In order to achieve the MPPT objective, one can seek that the error *e*1 is vanishing. To this end, the dynamic of *e*1 have to be clearly defined. Deriving (10), it follows from (6a) that:

$$\dot{e}_1 = -\frac{r}{L} i_d + \omega i_q + \frac{v_{pv}}{L} u_d - \frac{1}{L} e_{gd} - \dot{i}_{dref} \tag{11}$$

The goal, now, is to make *e*1 exponentially vanishing by Enforcing e_1 to behave as follows

$$\dot{e}_1 = -c_1 e_1 \tag{12}$$

where *c1 > 0* being a design parameter, Combining (11) and (12) the first control law is obtained,

$$u_d = \frac{L}{v_{pv}} \left(-c_1 e_1 + \frac{r}{L} i_d - \omega i_q + \frac{1}{L} e_{gd} + \dot{i}_{dref} \right) \tag{13}$$

The second control objective means that the grid currents *ia*, *ib* and *ic* should be sinusoidal and in phase with the AC grid voltage *ega* , *egb* and *egc* respectively. To this end the reactive power have to be null. According to (9b) the reference current *iqref* of *iq* should be zero (*iqref* = 0). The second following error is then introduced,

$$e_2 = i_q - i_{qref} \tag{14}$$

Its derivative, using (6b), is

$$\dot{e}_2 = -\frac{r}{L} i_q - \omega i_d + \frac{v_{pv}}{L} u_q - \frac{1}{L} e_{gq} \tag{15}$$

In order to achieve a power factor unit, one can seek that the error e_2 vanish exponentially. This amounts to enforcing its derivative e_2 to behave as follows

$$\dot{e}_2 = -c_2 e_2 \tag{16}$$

Where C2 >0 being a design parameter. Finally, combining (15) and (16), the second control law u_q can be easily obtained as follows

$$u_q = \frac{L}{v_{pv}} \left(-c_2 e_2 + \frac{r}{L} i_q + \omega i_d + \frac{1}{L} e_{gq} \right) \tag{17}$$

Since the two control laws *ud* and *uq* are clearly defined, the concern now is to ensure that the stability of the closed loop is fully ensured. This will be investigated in the next Subsection.

A. Stability analysis

The objective of the global stability of closed loop system can now be analyzed. This can be carried out by checking that the proposed controllers (13) and (17) stabilize the whole system with the state vector (*e*1,*e*2). To this end the following quadratic Lyapunov function is considered

$$V = \frac{1}{2} e_1^{\,2} + \frac{1}{2} e_2^{\,2} \tag{18}$$

Its derivative using (12) and (16) is obtained as follows

$$\dot{V} = -c_1 e_1^{\,2} - c_2 e_2^{\,2} \tag{19}$$

Which means that $V \cdot \leq 0$ and in turn shows that the equilibrium (*e*1,*e*2) =(0,0) of the closed loop system with the state vector (*e*1,*e*2) is globally asymptotically stable (GAS) [12]. This also means that, for any time *t*0 , and whatever the initial conditions (*e*1(*t*0),*e*2 (*t*0)) , one has

$$\lim_{t \to \infty} (e_1(t), e_2(t)) \to (0,0)$$

The main results of the paper are now summarized in the following proposition

Proposition

Consider the closed-loop system consisting of the system of Fig.1 represented by its nonlinear model (5a-b), and the controller composed of the control laws (13) and (17). Then, one has:
i) The closed loop system is GAS.
ii)The tracking error *e*1 vanishes exponentially implying MPPT achievement.
iii) The error *e*2 converges to zero implying the power factor unit.

4. Simulation Results

The theoretical performances of the proposed nonlinear controller are now illustrated by simulation. The experimental setup described in Fig.5, is simulated using MATLAB/SIMULINK. The injected currents to the grid have to be synchronized with the grid voltages. To this end a phase locked loop is used as can be seen from Fig.5. The characteristics of the controlled system are listed in Table IV. Note that the controlled system is

simulated using the instantaneous three phase model given by (5a-b). The model (6a-c) in d-q axis is only used in the controller design. The design parameters of the controller are given values of Table V. These parameters have been selected using a 'trial-anderror' search method and proved to be suitable. Fig.6 shows the block-diagram implementing the P&O algorithm that generates the reference current *idref*. The resulting closed loop control performances are illustrated by Fig.7 to Fig.12.

Parameter	Symbol	Value
PV array	PV power	70kW
DC link capacitor	C	3300µF
Grid filter inductor	*L, r*	3mH 0.2Ω
PWM	Switching frequency	10kHz
Grid	AC source Line frequency	220V 50Hz

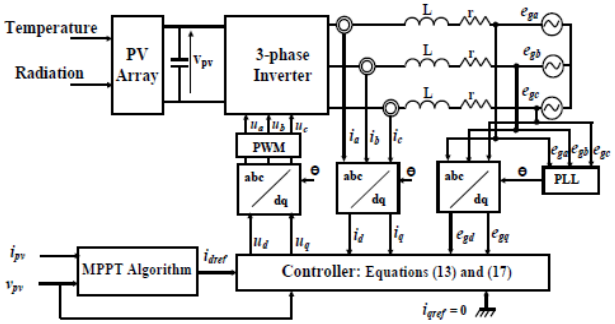

Fig.5: Simulation bench of the proposed three phase grid connected system

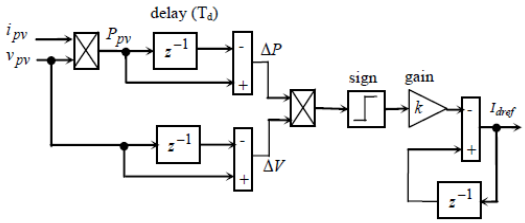

Fig.6: P&O algorithm implementation in Matlab/Simulink software

Table 5: Comptroller parameter

Parameter	Symbol	Value
Design parameters	*c*1	10^5
	*c*2	4×10^4
P&O algorithm parameters	Delay time Td	10^{-4}
	Step value k	0.3

A. change effect

Fig.7 shows the perfect MPPT in the presence of radiation step changes meanwhile, the temperature is kept constant, equal to 298.15K (25 °C). The simulated radiation profile is as follow: a first step change is performed between 600 and 1000W/m2 at time *t* =0.4s and the second one between 1000 and 800W/m2 at time *t* =0.8s. The figure shows that the PV power captured varies between (42.5kW) and (71.7kW) and then returns to (57.2kW). These values correspond (see Fig.3) to maximum points (M3, M1 and M2) of the curves associated to the considered radiation, respectively. The figure also shows that the voltage of the PV array *Vpv* varies between *Vpv* = 654.3V and *Vpv* = 664.2V and then returns to 661V, which correspond very well to the optimum voltages. Fig. 8 shows the injected currents *ia* and the grid voltage *ega* . This figure clearly shows that the grid current *ia* is sinusoidal and in phase with the grid voltage *ega* , proving that the power factor unit is achieved. The alternating currents injected to the grid are illustrated by Fig.9.

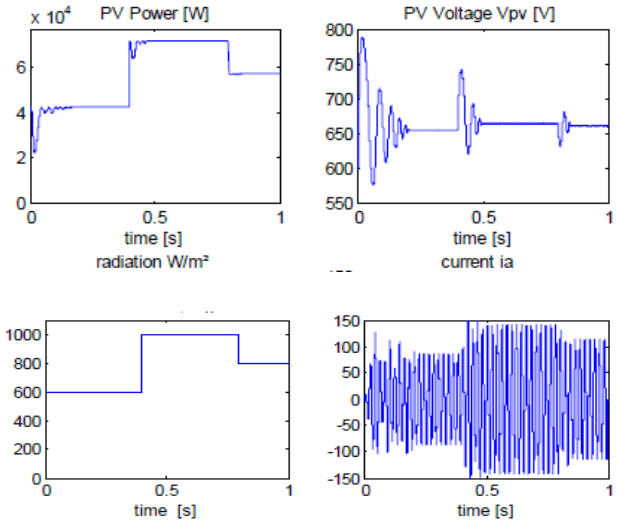

Fig.7: MPPT capability of the controller in presence of radiation step changes.

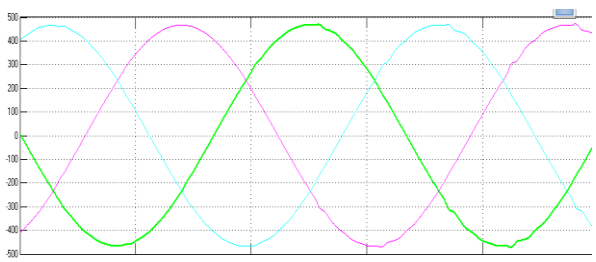

Fig 8. Voltage injected to Grid

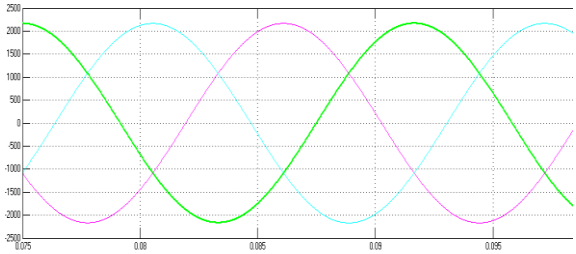

Fig 9. Current injected to Grid

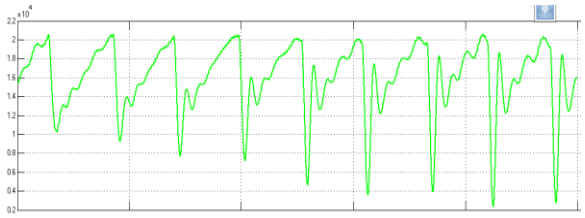

Fig 10. Current injected to Grid Active power supplied to grid

Conclusions

In this paper a three phase inverter for photovoltaic applications has been presented and controlled. The main feature of the presented system is it does not require an intermediate stage of DC-DC control, as the maximum power is set by the inverter itself by means of a Perturb & Observe algorithm. The system dynamics has been described by the nonlinear state-space model (5a-b). Based on a transformed model in d-q axis, a nonlinear controller defined by (13) and (17) is designed and analyzed using a Lyapunov approach. The controller objectives are threefold: i) ensuring the MPPT in the side of PV generator; ii) guaranteeing a power factor unit in the side of the grid, iii) ensuring the global asymptotic stability of the closed loop system. Using both formal analysis and simulation, it has been proven that the obtained controller meets all the objectives.

The authors can write the conclusion as a whole in a paragraph or by making points. An example is given as under.

1) Derivatives of the cooling curve can be used to understand the small changes in the under cooling of the liquids and solidus temperature.
2) Thermal analysis is a good technique to control carbides, shrinkage and micro-shrinkage formation.
3) It is visibly shown that there is significant reduction in undercooling degree on the alloys and the value of inoculation index was increased. Although the addition of Al,Ca,Zr-FeSipre-conditioners gives no significant influence .
4) The use of relative performance makes a clear distinction of the alloys efficiency and could be concluded that Ca,RE,S,O-FeSi inoculated iron gave the most influence.
5) From the result obtained, it could be deduced comparatively that Ca,RE,S,O-FeSi inoculant give the best efficiency followed by Ca,Zr-FeSi and Ca,Ba-FeSi inoculants respectively.

References

Barrade, P. Delalay, S. & Rufer A. (Apr. 2012), Direct connection of super capacitors to photovoltaic panels with on-off maximum power point tracking," IEEE Trans. Sustainable Energy, vol. 3, no. 2, pp. 283–294

Benavidas N. & Chapman, P., (Nov. 2005), Power budgeting famultiple-input buckboost converter, IEEE Trans. Power Electron., vol. 20, no. 6, pp. 1303– 1309.

Boldue, P.,Lehmicke, D. & Smith,J.,(1993) Performance of a grid connected PV system with Energy storage, in Proc. IEEE Photovoltaic Spec. Conf., pp. 1159–1162.

Bragard, M., Soltau, N., Doncker, R. W. D. & Schiemgel, A.(April 2010) Design and implementation of a 5 kW photovoltaic system with Li-ion battery and additional dc/dc converter, in Proc. IEEE Energy Convers. Congr. Expo., pp. 2944–2949.

Chiang, S. J., Chang, K. T. & Yen, C. Y.,(Jun1998)Residential photovoltaic energy storage system, IEEE Trans. Ind. Electron., vol. 45, no. 3, pp. 385–394.

Ding, F., Li, P., Huang, B., Gao, F., Ding, C. & Wang, C. (2010), Modeling and Simulation of grid connected hybrid PV/battery distributed generation system, in Proc. China Int. Conf. Electr. Distrib., pp. 1–10.

Doncker, R. W. D., Meyer, C., Lenke, R. U. & Mura, F. (Nov 2007),Power Electronics for future utility applications, in Proc. IEEE 7th Int. Conf. Power Electron. Drive Syst., , pp. K-1–K-8.

Enslin, J. H. & Snyman, D. B. , (Jan 1991),Combined low-cost, high efficient inverter,peak power tracker and regulator for PV applications, IEEETrans. Power Electron., vol. 6, no. 1, pp. 73–82.

Ertl, H. J., Kolar, W. & Zach, F. , (Oct. 2002)A novel multi cell dc-ac converter for applications in renewable energy systems, IEEE Trans. Ind. Electron., vol. 49, no. 5, pp. 1048–1057.

Ho, C., Breuninger, H., Pettersson, S., Escobar, G., Serpa, L. & Coccia, A.,(Jun. 2012), Practical design and implementation procedure of an interleaved boost converter using SiC diodes for PV applications, IEEE Trans. Power Electron., vol. 27, no. 6, pp. 2835–2845.

Hu, Y., Tatler, J. & Chen, Z. ,A , (Aug.2004),bidirectional DC/DC power electronic converter for an energy storage device in an autonomous power system, in Proc. IEEE Power Electron. Motion Control Conf., pp. 171– 176.

Auzani Jidin, NikIdris, Mohamed Yatim, (Sept Oct 2011), Simple Dynamic Over modulation Strategy For Fast Torque Control in DTC of Induction Machines With Constant-Switching-Frequency Controller IEEE transactions on industry applications, Vol. 47, No. 5.

Anthony Purcell, P. Acarnley,(may 2001.) Enhanced Inverter Switching for Fast Response Direct Torque Control, IEEE Transactions on Power Electronics, Vol. 16, No. 3

A. Mishra, P.Choudhary, (December 2012),Speed Control Of An Induction Motor By Using Indirect Vector Control Method, IJETAE,Volume 2, Issue 12.

B. K.Bose. (1997),. Power Electronics and Variable Frequency Drives. IEEE Press, New York.

Cristian Lascu, Boldea, Blaabjerg ,A (Feb 2000.) Modified Direct Torque Control for Induction Motor Sensorless Drive, IEEE transaction on Industry Applications, Vol.36, No.1.

E.Bassi, P. Benzi, S. Buja, (Oct. 1992) A Field Orientation Scheme for Current-Fed Induction Motor Drives Based on the Torque Angle Closed-Loop Control, IEEE Transactions on Industry Applications, Vol. 28, No. 5, Sept.

Ehsan Hassankhan, Davood A. Khaburi,(2008),DTC-SVM Scheme for Induction Motors Fed with a Three-level Inverter, World Academy of Science, Engineering and Technology.

Giovanna Oriti and Alexander L.Julian, (August 2011.)Three-Phase VSI with FPGA-Based Multisampled Space Vector Modulation, IEEE transactions on industry applications, Vol. 47, No. 4.

H. Arabaci and O. Bilgin,(June 2012), Squirrel Cage of Induction Motors Simulation via Simulink, International Journal of Modeling and Optimization, Vol. 2, No. 3.